Spatial and agronomic assessment of water erosion on inland Pacific Northwest cereal grain cropland

M. Samrat Dahal, J.Q. Wu, J. Boll, R.P. Ewing, and A. Fowler

Abstract: The inland Pacific Northwest (PNW) is characterized by high erosion rates attributed to hilly topography, highly erodible silt loam soils, wet winter seasons with frequent freeze-thaw events, and widespread use of conventional tillage practices. Historically, annual water erosion from cropland in the region's Palouse River basin averaged 20.6 t ha^{-1}, and more recent rates are 10, 13, and 11 t ha^{-1} for the low (<380 mm y^{-1}), intermediate (380 to 460 mm y^{-1}), and high (>460 mm y^{-1}) precipitation zones. Identifying source areas for targeted, effective management requires understanding the factors affecting water erosion, especially how tillage practices and crop rotation interact in various topographic, soil, and climatic settings. The objectives of this study were to (1) understand how hillslope hydrological and water erosion processes are influenced by key environmental factors (soil, climate, and topography) and management practices (tillage and crop rotation), and (2) assess the spatial distribution of soil erosion at the county level and by precipitation zone over the last 30 years. We compiled various combinations of soil, climate, topography, tillage, and crop rotation, and simulated these combinations county by county with the Water Erosion Prediction Project (WEPP) model. Simulated average annual erosion rates were lowest in the low-precipitation zone and highest in the intermediate-precipitation zone, exceeding the USDA Natural Resources Conservation Service tolerable limit (11 t ha^{-1}) in many cases. Temporally, high precipitation events and fallow periods in the rotation greatly increase erosion. Average annual erosion rates in Whitman County are 13.6, 19.0, and 15.4 t ha^{-1} in the three precipitation zones: low (<380 mm y^{-1}), intermediate (380 to 460 mm y^{-1}), and high (>460 mm y^{-1}), respectively. The intermediate-precipitation zone produced a total annual erosion of 4.2 × 10^6 t, despite having the smallest area. Columbia County has the highest erosion rate with 23.7 t ha^{-1} y^{-1}. Geospatial visualizations of the simulation results reveal critical source areas ("hotspots") where estimated erosion rates are more than five times the average rates, providing crucial information for, and advancing our understanding of, targeting management and increasing efficiency of conservation practices.

Key words: erosion hotspots—inland Pacific Northwest—water erosion—watershed modeling—WEPP

Soil erosion continues to be a major issue in cropland regions worldwide (Montanarella 2015), adversely impacting agricultural productivity and the environment by degrading soil and water quality (Lal 1998). From the mid-20th to early 21st century, soil erosion from conventionally tilled cropland globally has been one to two orders of magnitude greater than soil production (Montgomery 2007). Within the United States, annual soil erosion from cultivated cropland was evaluated every five years since 1982, and it was estimated to be 6.7 t ha^{-1} on average for 2017 (USDA 2020).

An example of a historically erosion-prone area is the inland Pacific Northwest (PNW), encompassing eastern Washington, northern Idaho, and northeastern Oregon. This area includes approximately 3.4 × 10^6 ha of dryland farming area (Papendick et al. 1983), and the main agricultural system is winter wheat (*Triticum aestivum* L.)-based (Schillinger et al. 2005). Hilly topography, highly erodible silt loam soils, a rainy and snowy winter season, and conventional tillage practices that leave surface soil pulverized and exposed all contribute to the area's high erosion rates (Papendick et al. 1983). The erosion process is dominated by winter events with frequent freeze-thaw cycles, which weaken soil aggregates and structures and render the soil susceptible to erosion (McCool and Roe 2005).

A 1978 USDA study conducted in the Palouse River basin of the inland PNW provided a comprehensive evaluation of the impact of water erosion on land and water quality. In Whitman County (southeastern Washington), which constitutes more than 50% of the Palouse River basin, soil loss was visually assessed in roughly 1,500 fields comprising 4.2 × 10^5 ha. The Universal Soil Loss Equation (USLE) (Wischmeier and Smith 1978) was used to estimate water erosion potentials for the dominant crop rotations in each precipitation zone. The study showed (1) from 1939 to 1977, annual water erosion from the cropland in the Palouse River basin averaged 20.6 t ha^{-1}, based on both visual assessment and the modified Alutin method (a simple approach using the cross-sectional areas of rills along a transect of specific length [Hill and Kaiser 1965; Hudson 1993]); (2) erosion rates varied widely during the study period, with the highest being 51 t ha^{-1} during the 1963 to 1964 season, and the lowest 1.3 t ha^{-1} during the unusually dry 1976 to 1977 season; (3) erosion rates estimated by the USLE for the tillage methods prevalent during the study period varied spatially, with annual averages of 29, 45, and 27 t ha^{-1} for the low-, intermediate-, and high-precipitation zones; and (4) the erosion potential from the USLE also varied by cropping system—

Mugal Samrat Dahal is a PhD student at Washington State University, residing at Puyallup, Washington. Joan Q. Wu is a professor at Washington State University, currently residing at Puyallup, Washington. Jan Boll is a professor at Washington State University, Pullman, Washington. Robert P. Ewing is a data scientist and soil scientist at The Climate Corporation, Seattle, Washington. Ames Fowler is a research associate in the Department of Earth and Environmental Sciences at Michigan State University, East Lansing, Michigan.

from 18 t ha⁻¹ for wheat–fallow to 38 t ha⁻¹ for wheat–barley (*Hordeum vulgare* L.)–fallow in the low-precipitation zone, 45 t ha⁻¹ for annual grain to 52 t ha⁻¹ for wheat–barley–fallow in the intermediate zone, and 9 t ha⁻¹ for eight-year rotation of wheat–peas (*Pisum sativum* L.)–alfalfa (*Medicago sativa* L.) to 25 t ha⁻¹ for wheat–barley–peas (WW–B–P) in the high-precipitation zone, all under conventional tillage.

The USDA Natural Resources Conservation Service (NRCS) has been recommending conservation practices for erosion reduction since the early 1930s (USDA NRCS 2020). Of those recommended practices, reduced tillage, direct seeding (no-till), and longer crop rotations have been adopted in many areas, including by some growers in the inland PNW starting in the early 1980s (Oldenstadt et al. 1982).

Solutions To Environmental and Economic Problems (STEEP), a USDA-sponsored research and education project, was established in 1975 to develop, and encourage growers to implement economically sound conservation cropping systems to combat erosion. STEEP lasted three decades and covered 3.4 × 10⁶ ha of rain-fed cropland across the three states of Washington, Idaho, and Oregon. Kok et al. (2009) reported the impact of conservation practices adoption during STEEP and assessed erosion potentials under alternative cropping systems in the three precipitation zones across the project area. Average erosion rate was estimated using the Revised Universal Soil Loss Equation (RUSLE2; USDA 2003). RUSLE2 simulations were performed for the three years (1975, 1990, and 2005) marking the beginning, middle, and end of the STEEP project. In the simulations for each precipitation zone, typical crop rotations and associated tillage practices (conventional or conservation) were varied while the climatic, topographic, and soil conditions were held constant. Percentage area under a specific crop rotation and tillage practices during each model year, estimated through grower interviews, were included in the erosion analysis as weighting factors. The simulated average annual erosion rates in 1975, 1990, and 2005 were 20, 14, and 10 t ha⁻¹ for the low-precipitation zone; 27, 16, and 13 t ha⁻¹ for the intermediate-precipitation zone; and 45, 24, and 11 t ha⁻¹ for the high-precipitation zone (Kok et al. 2009). Despite the increased implementation of conservation

practices, most of these erosion estimates still exceeded the soil loss tolerance level of 11 t ha⁻¹ (Soil Science Division Staff 2017) for the dominant soils in the study region.

Implementing conservation practices is complex and challenging. Mulla et al. (2008) found little evidence of water quality improvement at the watershed scale due to conservation projects. Possible reasons they suggested were the limited extent of best management practice (BMP) implementation and insufficient time from implementation to evaluation. Brooks et al. (2015) demonstrated that, for the inland PNW's Paradise Creek watershed, which is located in north-central Idaho, more than 30% of the total erosion was generated by as little as 1% of the watershed area, specifically those areas composed of shallow soils with steep slopes. They submitted that overall erosion from the watershed can best be reduced by targeting these critical areas. Such targeting requires detailed knowledge of how hydrology and erosion are affected by conservation practices in different topographic and geographic settings. One way to obtain this knowledge is by simulating various scenarios that combine the effects of climate, topography, and management with a model.

Process-based simulation models are useful in aiding management decision-making (Singh 1995). Such models allow for a better understanding of the hydrologic and erosion responses to changes in physical and management conditions. The USDA's Water Erosion Prediction Project (WEPP) is a distributed-parameter, continuous-simulation model for hydrology and erosion (Flanagan and Nearing 1995). The model simulates key hydrologic processes: runoff, infiltration, evapotranspiration (ET), subsurface lateral flow, and deep percolation, as well as soil freeze-thaw cycles and related winter hydrological processes. WEPP simulates erosion spatially and temporally due to both infiltration- and saturation-excess runoff (Pieri et al. 2007; Dun et al. 2009; Boll et al. 2015). The WEPP hillslope version, including its winter hydrology and erosion routines, has been tested in the inland PNW (Greer et al. 2006; Singh et al. 2009; Dun et al. 2010), and used to evaluate the impact on erosion of various tillage practices (Williams et al. 2010) in northeastern Oregon.

The increased availability and accessibility of spatially distributed physical and agronomic data (digital elevation model [DEM],

weather, land use, and management) enables broader-scale assessment of soil erosion and identification of critical source areas. County-by-county evaluation of water erosion as impacted by environmental factors and management decisions will help advance the understanding of relevant hydrological processes and inform extension and practice.

Objectives. This study aimed to assess water erosion from rain-fed cereal grain-based cropland in the eastern Washington portion of the inland PNW through WEPP simulation. The objectives were to (1) evaluate the relative effects of key environmental factors (soil, climate, and topography) and management practices (tillage and crop rotation) on hillslope hydrological and water erosion processes, and (2) assess the spatial, relative difference in soil erosion by county and by precipitation zone over the last 30 years (1989 to 2018).

Materials and Methods

Study Area. The study area encompasses the Washington counties of Douglas, Grant, Benton, Adams, Franklin, Lincoln, Spokane, Whitman, Walla Walla, Columbia, Garfield, and Asotin. Cereal grain-growing areas account for 54% of the total cropland in the study area (USDA NASS 2018; figure 1). Due to the wide variation in annual precipitation, the area is generally divided into three precipitation zones: high (>460 mm y⁻¹), intermediate (380 to 460 mm y⁻¹), and low (<380 mm y⁻¹) (Kok et al. 2009), with 3.0 × 10⁵, 2.7 × 10⁵, and 8.2 × 10⁵ ha of cereal grain respectively.

Climate. The climate in the study area varies from semiarid (Bsk) in the Columbia Plateau to Mediterranean (Dsb, Csa, Csb) in the eastern uplands, per the Köppen-Geiger classification (Kottek et al. 2006). Frontal weather systems carried by winds off the Pacific Ocean impact the climate, and a rain shadow effect is caused by Cascade Mountains in the west (Schillinger et al. 2005). The western part of the study area is the driest, receiving roughly 150 mm of precipitation annually. Precipitation increases gradually toward the east and reaches up to 630 mm in Whitman county (figure 2). Counties in the southeastern part of the study area (Whitman, Walla Walla, Columbia, Garfield, and Asotin) include all three precipitation zones (figure 2). Sixty to seventy percent of the total annual precipitation falls during November to April. In the north-
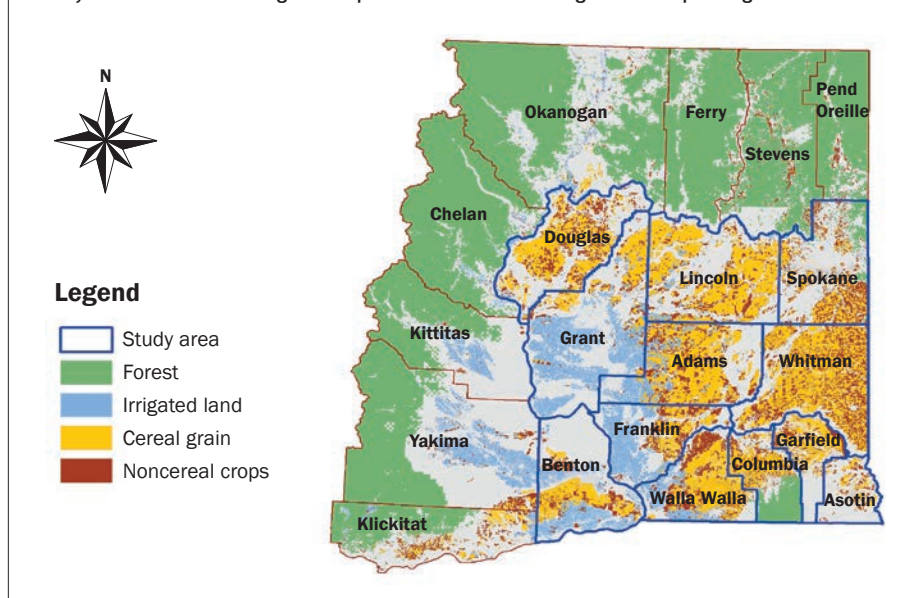
eastern part of the study area, where the elevation is higher, 20% to 25% of total precipitation is snowfall, and soil can freeze to a depth of 100 mm numerous times in a single season (Papendick et al. 1995). McCool and Roe (2005) reported 102 freeze-thaw cycles annually on average in Pullman, Washington, between 1971 and 2004. Climate data for the last 30 years (1989 to 2018) show that the warmest month with the highest average monthly maximum temperature was July (except for Whitman County where it was August), and the coolest month with the lowest monthly minimum temperature was December, with Grant being the driest county and Whitman the wettest (table 1).

Topography and Soil. The study area is underlain by basalt and characterized by undulating lands formed by sediment deposited by wind and water, with elevation ranging 80 to 1,950 m amsl (USGS 2019). Slope gradient was calculated from the 30 m resolution DEM for the study area obtained from USGS (2019) and processed using ArcMap (ESRI 2019). Slope gradient varies from flat to more than 45% (USGS 2019), with steep slopes predominant in the high-precipitation zone and flatter slopes toward the low-precipitation zone.

Percentage areas of slopes ≥20% for each county are included in table 1. Most soils in the study area are either Andisols formed from volcanic ash or Mollisols formed in loess deposits of windblown sediments (Shepherd 1985) with major soil series being Palouse and Nansene silt loam (Soil Survey Staff 2019). Soil texture is mostly silt loam (Papendick et al. 1995), and depth of loess deposits can reach up to 75 m in places (Busacca 1989).

Cropping Systems and Tillage Practices. Crop rotations adopted by farmers vary by precipitation zone, with the dominant systems being winter wheat–fallow (WW–F) in the low-precipitation zone, winter wheat–spring barley–fallow (WW–B–F) in the intermediate-precipitation zone, and WW–B–P in the high-precipitation zone (Kok et al. 2009). Summer fallow is used to store the winter precipitation, conserving soil water for planting the next crop in low- and intermediate-precipitation zones (Shepherd 1985). Tillage practices vary from farm to farm in the study area, recorded only as county-level aggregates. Intense tillage typically involves the use of moldboard plow, chisel plow, harrows, field cultivator, rod-

weeder, and double-disk drills (S. Johnson, personal communication, 2019). In recent decades, the use of heavy tillage equipment such as the moldboard plow has been reduced, and conservation tillage including no-till has been increasingly implemented (Kok et al. 2009; USDA NASS 2012, 2017) (figure 2a).

WEPP Inputs. WEPP hillslope simulation requires four major classes of inputs: climate, slope, soil, and management. The simulation period was chosen to be 1989 to 2018 to capture long-term water erosion as affected by variations in climate and management practices. We developed WEPP inputs for the cereal grain cropland (hereafter "model area") in the 12 counties in the study area.

Climate. For each precipitation zone in each study county, we obtained real daily precipitation and temperature data for 1989 to 2018 from either a weather station within the zone (if there is one) or the nearest station in the same precipitation zone in the nearest county (NCDC 2018). Missing data were filled with values from the nearest stations within the same precipitation zones following the inverse-distance-weighting method. Other WEPP climate inputs, such as dew-point temperature, wind speed and direction, and solar radiation were generated using CLIGEN (Nicks et al. 1995).

Slope. Following the slope classification of the *Soil Survey Manual* (Soil Science Division Staff 2017), we divided slope steepness within the study area into five levels (table 2). S1 and S2 are predominant, occupying 46.4%

and 20.4% of the study area, respectively. S5 occurs mostly on the rolling hills in the high-precipitation zone, accounting for 5.4% of the study area. The slope class distribution differs by county, with gentle slopes (S1 and S2) being more common in the low-precipitation zone (e.g., Grant, Benton, Lincoln, Adams, and Franklin counties), and steep slopes (S3, S4, and S5) mainly occurring in the high-precipitation zone (e.g., Whitman, Garfield, and Columbia counties) (figure 2b). For WEPP simulation, we set the length of the slope to 100 m, a middle value in the range of 10 to 200 m, slope length of numerous natural runoff plots across the United States where soil loss data had been collected (table 1 in Meyer 1982). We defined slope steepness at three slope positions (top, middle, and bottom) as WEPP inputs (table 2).

Soil. Soils were classified into three depth groups as shallow (<800 mm), moderate (800 to 1,200 mm), and deep (>1,200 mm) (figure 2c and table 3) by adapting the root-restricting depth classification from the *Soil Survey Manual* (Soil Science Division Staff 2017). Deep soils, common in all counties except Douglas and Asotin, cover 64.7% of the study area, whereas soils of moderate and shallow depth account for 8.0% and 27.3%, respectively (figure 2c).

For each county, we analyzed the soil data from the Soil Survey Geographic Database (SSURGO; Soil Survey Staff 2019) to obtain soil properties. Within each county, for each soil depth class, a representative total depth was defined by area-weighting the depths of

Figure 1
Study area: rain-fed cereal grain cropland in eastern Washington encompassing 12 counties.

Figure 2

(a) Precipitation zones (low [<380 mm y⁻¹]; intermediate [380 to 460 mm y⁻¹]; and high [>460 mm y⁻¹]) across the study area, and proportions of tillage practices in 2017 by county (USDA NASS 2017); (b) slope classes and distribution in each study county (USGS 2019); and (c) soil classes and distribution in each study county (Soil Survey Staff 2019).
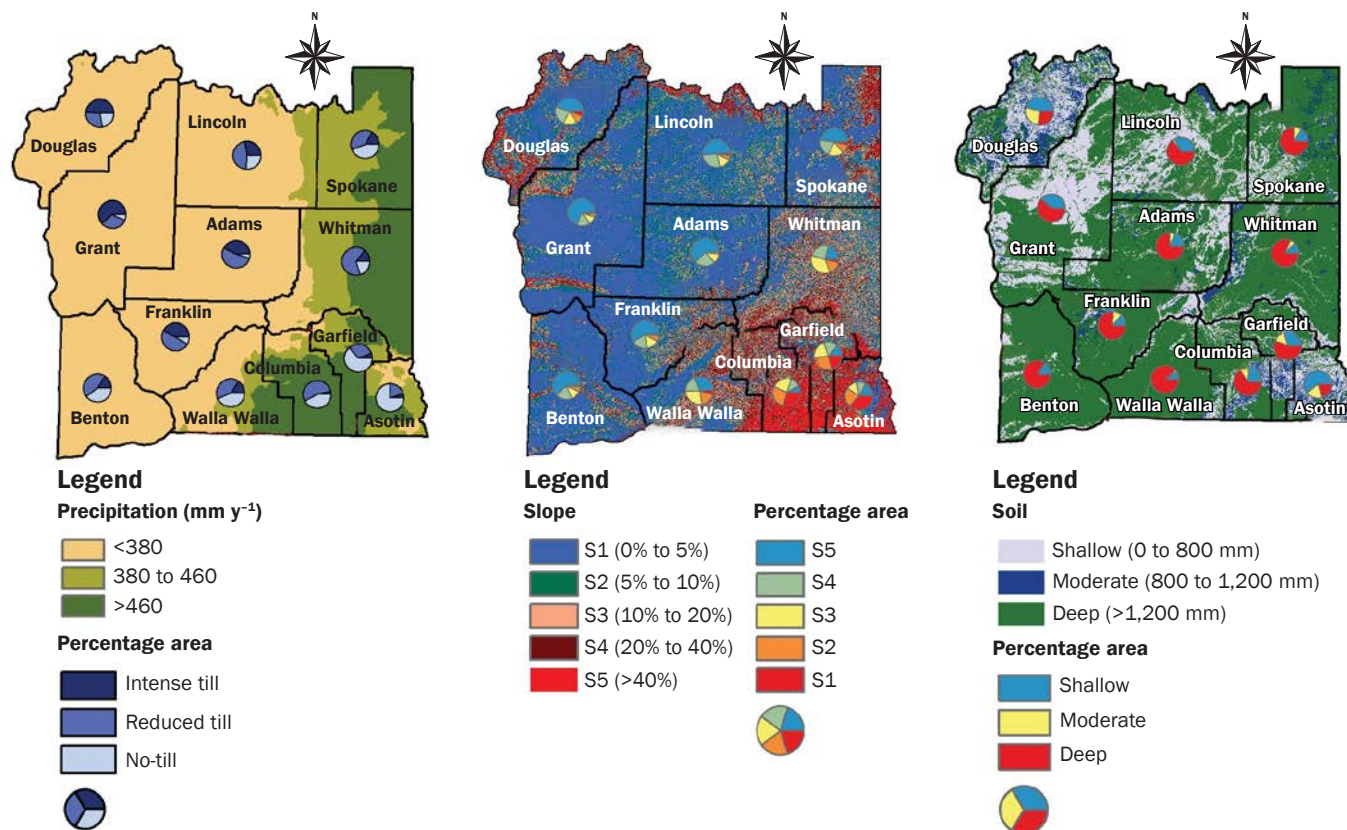

Table 1

Average temperature (°C) and precipitation (mm) during 1989 to 2018, by county, in the study area (NCDC 2018). Notice that not all counties contain all three precipitation zones.

County (area [×10⁴ ha]; percentage area of slope ≥20%)	Low				Intermediate				High			
	T_{max}	T_{min}	T_{mean}	P	T_{max}	T_{min}	T_{mean}	P	T_{max}	T_{min}	T_{mean}	P
Douglas (14.0; 1.0)	32.9	−5.2	10.7	269								
Grant (7.8; 0.3)	30.6	−4.8	10.5	197								
Benton (7.1; 1.6)	32.5	−3.2	11.6	210								
Adams (20.0; 1.6)	31.8	−4.1	10.3	259								
Franklin (5.1; 5.0)	31.7	−1.9	12.3	282								
Lincoln (25.0; 1.0)	29.3	−6.2	8.11	328	29.2	−4.9	9.0	419				
Spokane (7.0; 2.0)					29.2	−4.9	9.0	419	29.4	−4.8	8.83	457
Whitman (28.0; 14.0)	32.6	−4.7	10.1	384	30.0	−3.8	9.7	432	29.2	−3.9	9.0	516
Walla Walla (12.0; 20.7)	31.7	−1.9	12.3	282	32.3	−3.1	10.9	353	32.8	−1.3	12.6	478
Columbia (5.2; 25.4)	32.6	−4.7	10.1	384	32.3	−3.1	10.9	353	30.6	−2.7	10.6	472
Garfield (5.9; 10.3)	32.6	−4.7	10.1	384	30.0	−3.8	9.7	432	30.1	−3.7	10.1	465
Asotin (2.0; 2.0)	32.5	−1.8	11.9	323	30.0	−3.8	9.7	432	30.1	−3.7	10.1	465

Notes: T_{max} and T_{min}, average monthly maximum and minimum temperature. T_{mean} = mean daily temperature. P = average annual precipitation.

all soil series within the depth class, and the most prevalent soil series by percentage area was taken as representative of that county and depth class. The hydraulic properties of the representative soil series extracted from the SSURGO database, including the percentages of sand, clay, and organic matter, were used directly or with adjustment as WEPP soil inputs. Other soil inputs were taken from the literature or WEPP database, as further described below.

For all three soil depth classes, the soil profile was discretized into three layers (table 3). The depth of the first layer was set to 200 mm, typical of the depth of primary tillage. The depth of the second layer was set at roughly the middle of the soil profile: 300 mm for shallow soil and 600 mm for both moderate and deep soils. The depth of the third layer was the total depth of the representative soil series in each depth class for all counties.

The baseline hydraulic conductivity (K_b, mm s^{-1}), a crucial WEPP input subject to change due to soil freezing and tillage operation, was calculated following WEPP User Summary (Flanagan and Livingston 1995) (equations 1 and 2):

$$K_b = -0.265 + 0.0086 \times sand^{1.8} + 11.46 \times CEC^{-0.75}, \text{ for } clay \leq 40\% \text{, and} \quad (1)$$

$$K_b = 0.0066 \times e^{(244/clay)}, \text{ for } clay > 40\% \text{, } \quad (2)$$

where *sand* and *clay* are the percentages of sand and clay, and *CEC* (meq 100 g^{-1}) is the cation exchange capacity of the soil (*CEC* > 1 meq 100 g^{-1} for equation 1 to be valid).

The adjustment factors of thermal conductivity for unfrozen soil and snow were set to 0.5 and 1.5 following Dun et al. (2010). Adjustments were also made where the original input values were deemed unrealistic. For example, the soil organic matter content of 7% for the bottom soil layer in the moderate-depth soil class (Anders Kuhl complex soil) was adjusted to be within a more realistic range (<1.5%, 2% to 3%, and 3% to 4% for low-, intermediate-, and high-precipitation zones, respectively) (Schillinger et al. 2005; Kirby et al. 2017). The initial degree of saturation (actual soil water [mm] divided by soil water at saturation [mm] at the beginning of simulation) for each soil depth class in each precipitation zone was taken as the average initial saturation from multiple runs for dry, wet, and normal water years. For all

precipitation zones, the initial degrees of saturation ranged from 0.2 to 0.3 for shallow and moderate soil depths and 0.3 to 0.4 for deep soils.

Several crucial variables or parameters were given calibrated values. The K_h of the

restrictive layer was calibrated to 2 × 10^{-7} mm s^{-1} based on the range of the saturated K_h for unweathered and weathered basalt (2 × 10^{-8} to 4.2 × 10^{-4} mm s^{-1}; table 3.2 in Domenico and Schwartz 1997). Basalt is the predominant bedrock in the study region (Busacca

Table 2

Slope (percentage) classification, description, and inputs for Water Erosion Prediction Project (WEPP) simulation.

Slope class (%)	Description	Percentage area	Position along slope		
			Top	Middle	Bottom
S1 (0 to 5)	Nearly flat	46.4	2	5	2
S2 (5 to 10)	Gently sloping	20.4	3	10	3
S3 (10 to 20)	Strongly sloping	17.4	4	18	4
S4 (20 to 40)	Moderately steep	10.4	12	35	12
S5 (>40)	Steep	5.4	15	42	15

Figure 3

Overlay of slope (S1 [0% to 5%]; S2 [5% to 10%]; S3 [10% to 20%]; S4 [20% to 40%]; and S5 [>40%]), soil, and precipitation zone (low [<380 mm y^{-1}]; intermediate [380 to 460 mm y^{-1}]; and high [>460 mm y^{-1}]) in cereal grain cropland.
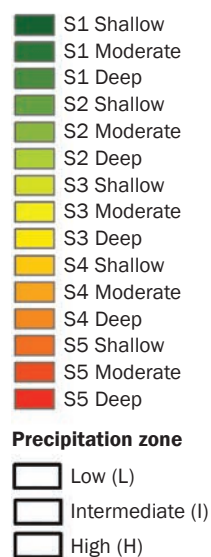

Table 3

Soil classes by depth (mm), and their layers.

Soil class	Depth (mm)		
	Layer 1	Layer 2	Layer 3
Shallow (<800 mm)	200	300	Area-weighted
Moderate (800 to 1,200 mm)	200	600	representative depth
Deep (>1,200 mm)	200	600	for the class

1989). The anisotropy ratio (horizontal to vertical hydraulic conductivity) was set to 1 for the first two soil layers and calibrated to 5 for the bottom layer. These parameter values produced an average annual ET as a percentage of annual precipitation (~80%) that was consistent with previous findings for winter wheat in the study region's high-precipitation zone (Cochran et al. 1982; Matsuura et al. 2021).

Three soil parameters for erosion computation in WEPP are the interrill erodibility (K_i [kg s m^{-4}]), the rill erodibility (K_r [s m^{-1}]), and the critical shear (τ_c [Pa]). Their baseline values can be calculated for the cropland soils following the WEPP User Summary (Flanagan and Livingston 1995). Rill erodibility and critical shear can differ markedly for unfrozen and thawing soils (Van Klaveren and McCool 1998). To represent the weakened state of soil experiencing frequent freeze-thaw cycles, we doubled the calculated values of both rill and interrill erodibilities (D. Flanagan, personal communication, 2019). We calibrated critical shear to one-tenth of the calculated value, which when applied to Whitman County under 100% intense tillage produced an average annual erosion rate compatible with the reported value prior to the implementation of conservation tillage (USDA 1978).

Important soil inputs for the deep soil in Whitman County, as an example, are shown in table 4. Input files for the three soil depth classes are included in supplemental tables S1 through S3. Baseline K_h for each soil layer in each depth class for all 12 study counties are presented in table S4.

Management. The USDA National Agricultural Statistics Service (NASS 2012, 2017) reports on types of tillage—intense, reduced, and no-till—and the percentage of each type for all croplands in each county of Washington State (figure 1). With the assumption that the proportions for each practice are the same for cereal grain cropland as for all cropland, we created nine management files combining three tillage types and three crop rotations associated with the three precipitation zones. Management inputs related to tillage implementation, including the number of passes and type of equipment as well as the timing of planting and harvest, were taken from WEPP database and adjusted based on literature and in consultation with USDA NRCS staff (S. Johnson, personal communication, 2019).

Tillage depths were adjusted from the default values in the WEPP database for different tillage intensities and equipment representative of the study region. For intense tillage, heavy equipment such as a twisted point chisel plow or moldboard plow was used for primary tillage. For reduced tillage, the heavy equipment was omitted and the number of passes per crop was decreased. The fractions of residue buried (T_i) for different tillage operations were taken from the WEPP documentation (table 9.5.1 in Flanagan and Nearing [1995]). For the drier areas, we set the seeding spacing to be wider because less soil water is available. The resultant row width was 0.18 m for the high-precipitation zone, 0.305 m for the intermediate-precipitation zone, and 0.38 m for the low-precipitation zone. Major management inputs for intense tillage and WW−B−P rotation, as an example, are shown in table 5. Major input parameters from all nine management input files for the three precipitation zones (or crop rotations) and three tillage practices for WEPP simulations are included in tables S5 through S13.

WEPP Simulations. WEPP version 2012.8 was used for the 30-year simulations, with hourly infiltration computation. Overlaying the classified maps of slope steepness, soil depth, and precipitation zone (crop rotation) yielded 45 "subareas" (figure 3), each representing a unique combination of the three factors, not all of which may be present within a given county. Adding consideration of three

Table 4
Major soil properties for deep soil (Palouse silt loam) in Whitman County.

Description	Value
Texture	Silt loam
Number of model soil layers	3
Albedo	0.16
Surface K_h (mm h^{-1})	1.9
Initial saturation of soil porosity (m^3 m^{-3})	0.4
Baseline interrill erodibility (kg s m^{-4})	9.8×10^6
Baseline rill erodibility (s m^{-1})	0.0178
Baseline critical shear (N m^{-2})	0.35
Depth to the restrictive layer (m)	1.8
Restrictive layer hydraulic conductivity (mm s^{-1})	2.9×10^{-6}

Table 5
Major management inputs used for intense tillage with wheat−barley−pea rotation.

Parameter	Value
Ridge height value after tillage (m)	0.075
Ridge interval (m)	0.30
Fraction of residue buried by chisel plow*	0.65
Fraction of residue buried by moldboard plow*	0.80
Depth of tillage for chisel and moldboard plow (m)	0.20
Depth of tillage for spike tooth harrow (m)	0.076
Random roughness value after tillage (m)	0.025
Fraction of surface area disturbed	1.0
Row width (m)	0.18
Maximum canopy height for winter wheat (m)	1.0
Canopy cover coefficient for winter wheat	5.2
Initial ridge height after last tillage (m)	0.08
Initial ridge roughness after last tillage (m)	0.05
Initial snow depth (m)	0.0
Initial frost depth (m)	0.0
Initial total dead root mass (kg m^{-2})	0.4

*Taken from table 9.5.1 of Water Erosion Prediction Project (WEPP) documentation (Flanagan et al. 1995).

types of tillage led to a total of 135 ($i \times j \times k \times l$, where $i = 5, j = 3, k = 3$, and $l = 3$) scenarios for WEPP simulation (table 6). These simulations were repeated for each of the 12 counties in the study area. Annual and 30-year average outputs for water balance and erosion rate were obtained. R scripts were written to automate various steps of preprocessing (e.g., batch and run file creation) and postprocessing (e.g., for water balance and erosion results, calculating total areas of the subareas sorted by different criteria).

Analysis of Results. To estimate annual (and thence 30-year average) countywide erosion, we first estimated the proportions of the three tillage types for each county. The USDA NASS (2012, 2017) tillage data are available for only two years, so linear interpolation and extrapolation (equation 2) were used to fill in tillage practices for other years of the study. Estimated annual fractions of the three tillage types for Whitman and Garfield counties, as examples, are shown in table 7. This information for the remaining 10 counties is given in table S14.

$$r_{t \pm 1} = r_t \pm \frac{r_{2017} - r_{2012}}{5} , \qquad (3)$$

$$n_{t \pm 1} = n_t \pm \frac{n_{2017} - n_{2012}}{5} , \text{ and} \qquad (4)$$

$$i_t = 100 - (r_t + n_t) , \qquad (5)$$

where r_t, n_t, and i_t are respectively the percentages of reduced, no-, and intense tillage (all ≥ 0), and t is the year index (2018, 2016 to 2013, and 2011 to 1989). The minus cases apply to the year 1989 to 2011. Note that r_t, n_t, and i_t are known for years 2012 and 2017, and that the percentages of the three tillage types add to 100.

Denote as a_{ijk} the subarea (ha, as described earlier) of a county that has the unique combination of slope i, soil depth j, and crop rotation k. Further, denote as e_{lijk} the annual (or 30-year average) erosion rate (t ha^{-1} y^{-1}) for this subarea under tillage $l, l = 1, 2, 3; f_l$ the annual (or 30-year average) fraction of tillage type l for the county; and A the total area for all the unique combinations in the county.

We assumed that county-level tillage proportions reported for all crops (USDA NASS 2012, 2017) hold true for cereal grain cropland, and also for each subarea. The countywide annual (or 30-year average) erosion rate E (t ha^{-1} y^{-1}) is then

Table 6
Water Erosion Prediction Project (WEPP) simulations combining slope and soil depth classes, tillage types, and crop rotations.

Index	Slope *i* (%)	Soil depth *j* (mm)	Crop rotation* *k*	Tillage *l*
1	S1 (0 to 5)	Deep (>1,200)	WW–B–P (high-precipitation zone)	Intense
2	S2 (5 to 10)	Moderate (800 to 1,200)	WW–B–F (intermediate-precipitation zone)	Reduced
3	S3 (10 to 20)	Shallow (<800)	WW–F (low-precipitation zone)	No-till
4	S4 (20 to 40)			
5	S5 (>40)			

*Crops in the rotations are winter wheat (WW), barley (B), pea (P), and fallow (F).

Table 7
Annual percentages of intense, reduced, and no-till.

Year	Whitman County Intense	Reduced	No-till	Garfield County Intense	Reduced	No-till
2018	12.0	67.9	20.0	1.7	30.0	68.2
2017*	14.8	65.2	20.0	6.3	30.9	62.9
2016	17.6	62.5	19.9	10.8	31.7	57.5
2015	20.4	59.8	19.8	15.4	32.6	52.1
2014	23.2	57.0	19.8	19.9	33.4	46.7
2013	26.0	54.3	19.7	24.5	34.2	41.3
2012*	28.8	51.6	19.6	29.0	35.1	35.9
2011	31.5	48.9	19.6	33.6	35.9	30.5
2010	34.3	46.2	19.5	38.1	36.8	25.1
2009	37.1	43.5	19.4	42.7	37.6	19.7
2008	39.9	40.7	19.4	47.2	38.4	14.3
2007	42.7	38.0	19.3	51.8	39.3	8.9
2006	45.5	35.3	19.2	56.4	40.1	3.5
2005	48.3	32.6	19.2	60.9	39.1	0.0
2004	51.0	29.9	19.1	65.5	34.5	0.0
2003	53.8	27.1	19.0	70.0	30.0	0.0
2002	56.6	24.4	19.0	74.6	25.4	0.0
2001	59.4	21.7	18.9	79.1	20.9	0.0
2000	62.2	19.0	18.8	83.7	16.3	0.0
1999	65.0	16.3	18.8	88.2	11.8	0.0
1998	67.8	13.6	18.7	92.8	7.2	0.0
1997	70.5	10.8	18.6	97.3	2.7	0.0
1996	73.3	8.1	18.6	100.0	0.0	0.0
1995	76.1	5.4	18.5	100.0	0.0	0.0
1994	78.9	2.7	18.4	100.0	0.0	0.0
1993	81.7	0.0	18.3	100.0	0.0	0.0
1992	81.7	0.0	18.3	100.0	0.0	0.0
1991	81.8	0.0	18.2	100.0	0.0	0.0
1990	81.9	0.0	18.1	100.0	0.0	0.0
1989	81.9	0.0	18.1	100.0	0.0	0.0
30-year average	51.5	29.4	19.1	63.0	21.5	15.5

*Data for 2012 and 2017 reported by the USDA National Agricultural Statistics Service were used to interpolate and extrapolate for other years.

$$E = \frac{1}{A} \times \sum_{l=1}^{3} f_l \sum_{i=1}^{5} \sum_{j=1}^{3} \sum_{k=1}^{3} e_{lijk} \times a_{ijk}. \quad (6)$$

Annual and 30-year average erosion rates and water balances for hillslopes (excluding channels) by county and precipitation zone were obtained and evaluated to elucidate the effects of slope, soil depth, and crop rotation on water erosion for representative counties.

Results and Discussion

Erosion Rate and Total Amount by County and Precipitation Zone. All the erosion rates and total amount presented below are for the hillslopes of cereal grain cropland of the study area. In general, the intermediate-precipitation zone generally produces the highest erosion rates and a large amount of erosion (table 8). The chief contributors to this high quantity of erosion are the fallow period after barley harvest when the ground has little residue, and the greater precipitation and runoff than in the low-precipitation zone. In contrast, fallow that leaves the soil surface exposed is not practiced in the high-precipitation zone.

Hillslope erosion, in terms of both simulated rate and total amount, varies county by county and by precipitation zone. Within the high-precipitation zone, Whitman County has the highest amount of annual erosion at 2.3×10^6 t, and Columbia County has the highest simulated 30-year average erosion rate at 23.7 t ha^{-1}. Garfield County also has high average erosion rates due to its relatively steep topography, though low total erosion because of its small cereal grain-growing area. Comparing Walla Walla and Columbia with similar topography (areas of slopes ≥20% accounting for 21% and 25%) but different tillage practices (percentage intense tillage 43% and 59%), overall erosion rates in the former (6.6 t ha^{-1}) are much lower than in the latter (22.1 t ha^{-1}). On the other hand, erosion rates in Asotin County are lower than all neighboring counties as the county has the highest percentage area under no-till. Erosion rates in the low-precipitation zone are primarily low due to the low precipitation and runoff generation.

In many counties the average simulated erosion rate is relatively low, and yet the maximum erosion rate may be quite high (table 9). The average erosion rates tend to be skewed toward the lower values, because most of the area has gentle slopes. Asotin County had the highest area-weighted stan-

dard deviation, 57.8 t ha^{-1} y^{-1}, within the intermediate-precipitation zone. The standard deviation varies substantially across counties, even among those in the same precipitation zone, because of the differences in topographic and soil conditions as well as tillage practices. In counties such as Douglas and Grant, the maximum erosion rate as a result of combined steep slope, shallow soil, and intense tillage is more than five times the average rate.

Compared to the current level, total erosion amount would increase by 52% if the whole model area would be under intense tillage, or it would decrease by 45% or 81% if the reduced tillage or no-till would be fully implemented. Four scenarios of WEPP-simulated 30-year average erosion rates for all subareas are shown in figures 4a through 4d. These maps illustrate the spatially varying erosion rates, including the "hotspots" with elevated erosion rates where conservation management could be most effectively targeted. Erosion hotspots generally appear in areas with high (>460 mm) and intermediate (380 to 460 mm) annual precipitation within the study area, as those areas produce greater runoff. More hotspots appear in the intermediate-precipitation zone, as the fallow year in the WW-B-F rotation leads to more erosion. Areas with steeper slopes are often identified as erosion hotspots, especially when they are under intense tillage. Notably, more spatially explicit results would result if tillage practice data had been available at a finer resolution than the county level.

Effects of Slope, Soil Depth, Tillage, and Crop Rotation. A clear trend in the simulation results is that erosion rates decrease with decreasing slope steepness and tillage intensity. In order to understand the effect on water erosion of each individual factor in isolation, we aggregated the WEPP simulation results by county within each class of every factor (e.g., slope) and then calculated the averages for each class. The effects of individual factors on water erosion are illustrated in figure 5.

The effect of soil depth does not follow a clear trend like slope steepness and tillage. This is because various other soil properties, such as K_b, soil erodibility, and critical shear stress, also influence runoff and erosion. The winter WW−F rotation has the lowest erosion rate, but only because this rotation is implemented in the low-precipitation zone with low runoff.

WEPP Results for Whitman County. In Whitman County, average annual simulated erosion rates are 13.6, 19.0, and 15.4 t ha^{-1} in the low-, intermediate-, and high-precipitation zones, respectively. These values are slightly higher than those reported by Kok et al. (2009) based on RUSLE2 simulation, i.e., 10, 13, and 11 t ha^{-1} for the respective zones. We examined the WEPP simulation results for Whitman County where all three precipitation zones (and crop rotations) are present, in order to better understand how hydrologic and erosion processes are affected by topography, soil, and crop rotation.

WEPP-simulated ET and runoff generally decrease as annual precipitation and soil

Table 8

Thirty-year average area-weighted erosion rate (t ha^{-1} y^{-1}) and total amount (t) in parentheses by county and precipitation zone.

County	Precipitation zone			Countywide
	Low	Intermediate	High	
Douglas	1.9 (2.6 × 10⁵)			1.9 (2.6 × 10⁵)
Grant	3.5 (2.8 × 10⁵)			3.5 (2.8 × 10⁵)
Benton	1.3 (9.1 × 10⁴)			1.3 (9.1 × 10⁴)
Adams	1.6 (3.1 × 10⁵)			1.6 (3.1 × 10⁵)
Franklin	2.1 (1.1 × 10⁵)			2.1 (1.1 × 10⁵)
Lincoln	7.8 (1.7 × 10⁶)	14.2 (4.8 × 10⁵)		8.6 (2.2 × 10⁶)
Spokane		11.4 (3.0 × 10⁵)	6.6 (2.9 × 10⁵)	8.4 (5.9 × 10⁵)
Whitman	13.6 (2.7 × 10⁵)	19.0 (2.2 × 10⁶)	15.4 (2.3 × 10⁶)	16.7 (4.7 × 10⁶)
Walla Walla	2.0 (7.9 × 10⁴)	10.1 (4.4 × 10⁵)	7.7 (2.6 × 10⁵)	6.6 (7.8 × 10⁵)
Columbia	16.7 (6.0 × 10⁴)	17.5 (1.6 × 10⁵)	23.7 (9.3 × 10⁵)	22.1 (1.1 × 10⁶)
Garfield	19.0 (5.5 × 10³)	21.5 (5.7 × 10⁵)	16.6 (5.4 × 10⁵)	18.8 (1.1 × 10⁶)
Asotin	2.2 (8.7 × 10³)	8.4 (1.2 × 10⁵)	2.9 (4.7 × 10³)	6.8 (1.4 × 10⁵)
All counties	3.8 (3.2 × 10⁶)	15.8 (4.2 × 10⁶)	14.4 (4.3 × 10⁶)	8.4 (1.2 × 10⁷)

Table 9
Descriptive statistics of average area-weighted erosion rate (t ha^{-1} y^{-1}).

County	Low-precipitation zone				Intermediate-precipitation zone				High-precipitation zone			
	Min.	Mean	Max.	Std.	Min.	Mean	Max.	Std.	Min.	Mean	Max.	Std.
Douglas	0.1	1.9	35.6	6.9								
Grant	0.2	3.5	49.6	10.5								
Benton	0.1	1.3	17.0	4.2								
Adams	0.1	1.6	26.2	6.7								
Franklin	0.0	2.1	12.1	2.7								
Lincoln	0.3	7.8	72.1	17.8	0.3	14.2	97.1	20.8				
Spokane					0.5	11.4	104.0	23.2	0.1	6.6	64.8	18.0
Whitman	0.2	13.6	55.7	16.3	0.2	19.0	78.4	20.6	0.0	15.4	84.4	23.5
Walla Walla	0.05	2.0	12.1	2.9	0.3	10.1	41.8	10.0	0.0	7.7	36.9	10.6
Columbia	0.2	16.7	84.2	22.4	0.4	17.5	67.3	16.6	0.1	23.7	118.0	28.4
Garfield	0.2	19.0	106.0	31.0	0.2	21.5	128.0	33.6	0.3	16.6	125.0	31.4
Asotin	0.0	2.1	44.8	11.3	0.1	8.38	257.0	57.8	0.1	2.9	112.0	24.1

Table 10
Annual water balance (mm) for slope class S3 (10% to 20%) and intense tillage. In parentheses are percentages of the sum of annual rainfall and snowmelt.

Precipitation zone	Soil depth	Rainfall and snowmelt	Runoff	Deep percolation	Evapotranspiration	Lateral flow
High	Deep	518 (100)	80 (16)	0 (0)	434 (83)	0 (0)
	Moderate	518 (100)	63 (12)	4 (1)	406 (78)	42 (8)
	Shallow	518 (100)	69 (12)	4 (1)	402 (78)	39 (8)
Intermediate	Deep	436 (100)	53 (12)	1 (0)	374 (86)	1 (0)
	Moderate	436 (100)	34 (8)	4 (1)	341 (78)	51 (12)
	Shallow	436 (100)	39 (9)	5 (1)	343 (79)	44 (10)
Low	Deep	388 (100)	59 (15)	0 (0)	321 (83)	0 (0)
	Moderate	388 (100)	41 (11)	4 (1)	304 (78)	32 (8)
	Shallow	388 (100)	36 (9)	5 (1)	299 (77)	42 (11)

depth decrease (table 10). ET and runoff account for the majority (86% to 98%) of annual water balance, and deep percolation is negligible. The decrease in ET with decreasing precipitation and soil depth is due to a lack of plant-available water. The decreased runoff with decreasing precipitation can likewise be attributed to low precipitation. On the other hand, the low-precipitation zone produced slightly more runoff than did the intermediate-precipitation zone, because the fallow period in alternate years of the WW–F crop rotation preserves and thereby increases soil water. As a result, precipitation events early during the wheat crop generate more runoff. The same reasoning explains the typically higher lateral flow in the lower precipitation zones relative to the high-precipitation zone: more accumulation of soil water occurs during the fallow year.

Within a precipitation zone, ET and runoff mostly decrease as lateral flow increases with decreasing soil depth (table 10). The simulated lateral flow is greater for the shallower soils where the infiltrated water can reach the restrictive layer faster and leave via rapid lateral movement (anisotropy ratio 5).

Erosion hotspots occur in all three precipitation zones, with 59%, 57%, and 54%, respectively, of the hillslopes in the low–, intermediate–, and high-precipitation zones having erosion rates greater than the NRCS soil loss tolerance level. Figure 6 shows a map overlay of classified soil slope and depth with precipitation zone, together with spatial distribution of average erosion rate. Had finer-resolution tillage data been available, the spatial distribution of erosion could have been better quantified and visualized. Erosion maps for the other 11 counties are

presented in supplementary information S5. Future conservation management focusing on areas of high erosion rates shown in these erosion maps would be more cost-effective in reducing overall erosion as suggested in previous studies (Brooks et al. 2015).

Temporally, simulated erosion depends on county-level tillage intensity partitioning, annual precipitation, and crop rotations. Starting the WEPP simulation at a different year of the crop rotation would give different erosion results for each individual year due to interactive effects between crop, soil, and weather conditions (e.g., timing of precipitation events). In reality, all fields within a given precipitation zone would not necessarily be in the same phase of the rotation year. Nonetheless, the long-term average annual erosion would not change markedly even if the fields were distributed across different

Figure 4

Average erosion (a) weighted by county-level fractions of tillage types (intense, reduced, and no-till) following USDA National Agricultural Statistics Service (NASS) data, and for the hypothetical cases that all cereal grain cropland is under (b) intense, (c) reduced, and (d) no-till, in the three precipitation zones: low (<380 mm y^{-1}); intermediate (380 to 460 mm y^{-1}); and high (>460 mm y^{-1}).
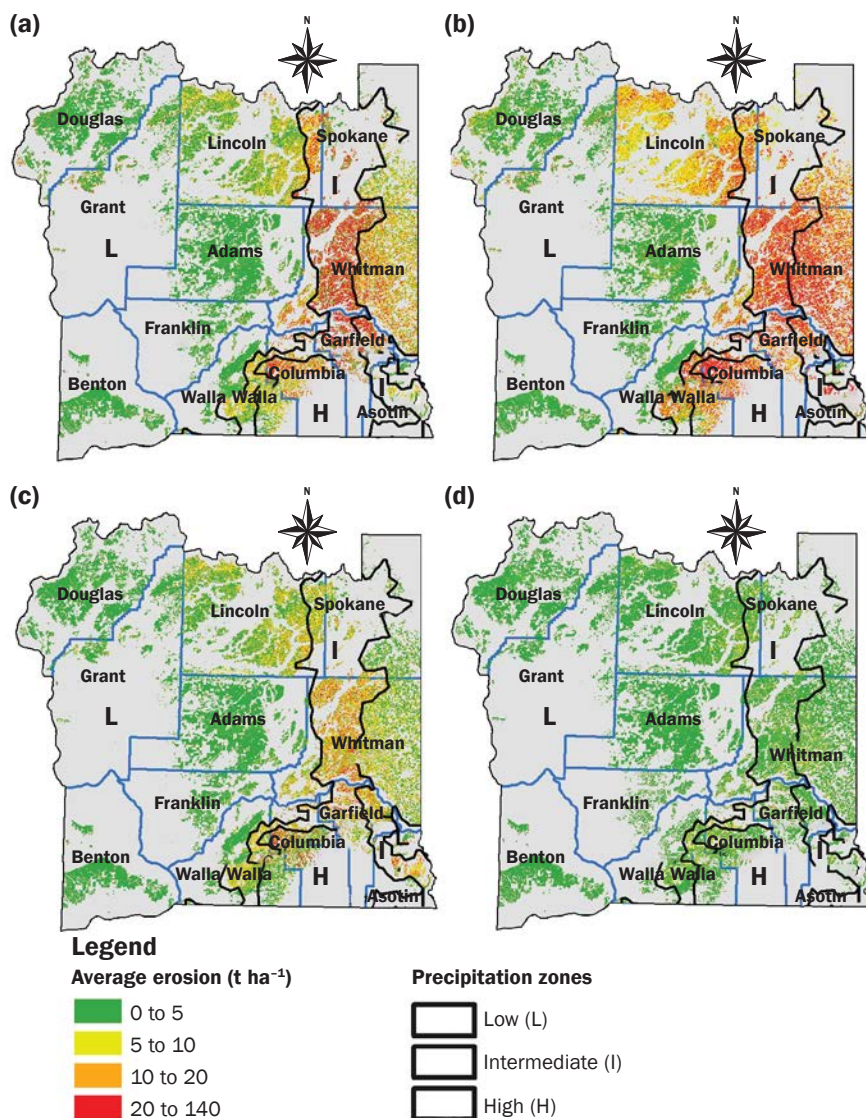
phases of the crop rotation every year. For instance, there would be more tillage passes for the wheat phase, and fewer for pea, resulting in greater erosion in the wheat fields and less erosion from the pea fields. The condition would be reversed the following year, and over the long run the effect of fields being under different crop rotation phases would be smoothed out.

Erosion decreases as the fraction of intense tillage decreases year by year. We used the inferred annual partitioning of tillage practices in obtaining yearly average erosion rate to examine its temporal variation in Whitman County (figure 7). Annual erosion rates for the other 11 counties are included in supplementary information S6. The high erosion rates generally occur in the winter wheat portion of the crop rotation, as the preplanting tillage increases the soil erodibility before the winter. In the barley and pea portions of the rotation, soil erosion is not as high because the crop is harvested shortly before fall, after which the soil is protected from winter rains by the barley and pea residue. In the fallow year, soils are bare and comparatively more vulnerable to erosion. The fallow and win-

ter wheat years, if combined with extreme precipitation events, can produce extremely high erosion as in years 1993, 1997, and 2017 in the low-; 1991, 1994, 2006, and 2009 in the intermediate-; and 1994 and 2015 in the high-precipitation zone.

Erosion rate spiked in 2006 at the intermediate-precipitation zone due to (1) above-average winter precipitation resulting in more runoff events and larger runoff volume, and (2) rainfall-runoff events on recently tilled and thawing soil coinciding with a wheat-planting year. Such a spike did not happen for the high-precipitation zone because the pea crop preceding wheat uses soil water, leading to a lower degree of saturation (~40%) and less runoff than occurred in the intermediate precipitation zone. There, the fallow year preceding wheat allows more soil water to accumulate, resulting in a higher degree of saturation (~55%) and more runoff. The erosion rate did not peak that year for the low-precipitation zone because of the low winter precipitation and lower degree of saturation (~50%). The "hot flash" years with high erosion should also be targeted for erosion control given the improvement in short-term predictability of climate (DiNezio et al. 2017; Tang et al. 2018), especially La Niña years that typically produce wetter-than-average winters in the PNW (Taylor 1998), such as 2009 and 2017 (Zhang et al. 2019).

Cover crops may be planted in fallow years for protection against soil erosion (Langdale et al. 1991). Use of cover crops may be hindered by low soil water availability for the subsequent crop, especially in dryland regions, but their integration combined with conservation tillage can improve agroecosystem performance over time (Ghimire et al. 2018). For example, in the United States triticale has gained popularity as forage or a cover crop (Ayalew et al. 2018) and has been shown to increase the net profitability of agriculture systems in the drylands of central Great Plains when it replaces fallow under wheat–corn (*Zea mays* L.)–fallow rotation (Nielsen et al. 2017). Adoption of regenerative management practices and diverse cropping system with less frequent fallow has been initiated in the PNW (Huggins et al. 2015).

Runoff decreases with decreasing tillage intensity, as expected. Increased slope steepness increases the simulated runoff, except for shallow soil (figure 8). In shallow soils, WEPP-simulated lateral flow increases pre-

cipitously with increase in slope steepness because the infiltrated water would reach the bottom layer faster than in deep soils, and the combined effect of anisotropy (ratio of 5) and large slope gradient cause water to transmit laterally out of the soil profile quickly. As such, the soils of shallow depths and steep gradients are unsaturated more frequently and produce less runoff than those of larger depths.
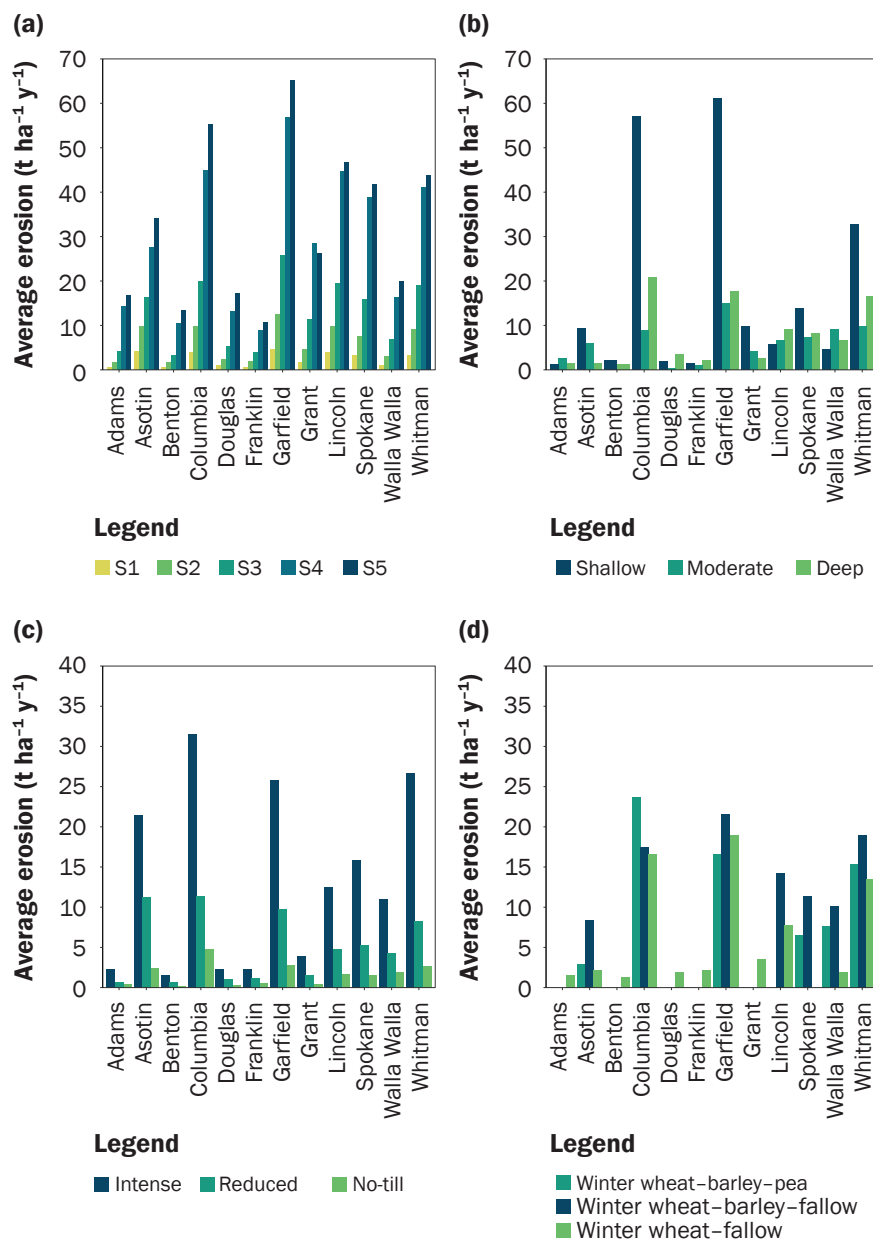
Decreasing tillage intensity reduces erosion mainly because reduced tillage leaves residue on the surface, providing a cover resistant to erosion even on steep slopes. For example, in the high-precipitation zone, erosion decreased by more than a factor of four on S1 and S2 slopes due to the change from intense tillage to reduced tillage (figure 9). As discussed in "Erosion Rate and Total Amount by County and Precipitation Zone," the WW–B–F rotation generally yielded a greater erosion rate than WW–B–P and WW–F, except for the shallow soils on steep slopes S4 and S5. This decrease in erosion rate on steep slopes was due to the increase in lateral flow and thus decrease in runoff. The combination of a shallow soil on less steep slopes and low K_h (table S3) leads to higher saturation-excess runoff and causes the greatest erosion rates within the county.

Consider for example a WEPP run for slope class S3 (moderate slope), deep soil, intense tillage, and a WW–B–P rotation. Annual precipitation and average erosion rate for the 30-year simulation are illustrated in figure 10. The years 6 and 27, during which winter wheat is planted, yield the highest rate of erosion, although year 8 receives the highest precipitation. In year 6, much of the precipitation occurs during the fall-winter season following winter wheat planting. Early in the rainy season, before the wheat has germinated, the soil has no protection from residue or a living crop. Furthermore, preplanting tillage for seedbed preparation increases soil erodibility. As a result, the precipitation events, especially the rain-on-thawing-ground type, can cause high erosion. In year 8, there is adequate residue cover on the ground from pea harvest and no preplanting tillage that increases soil erodibility.

We further examined WEPP-simulated water balance, erosion, and winter processes for year 6 for the same scenario, which yields the second-highest annual erosion rate (figure 11) of 93.8 t ha⁻¹. Much of the erosion hap-

pens after winter wheat planting has occurred. During this time of the year, the seeds are yet to be germinated, and the land surface is essentially bare. As a result, the soil is prone to erosion during rain and snowmelt events. Runoff events occur on days 334, 335, 336, and 353, but not all events result in erosion because the soil is frozen at times, e.g., the rain event on day 329 produces runoff but not erosion as the soil is frozen.

Major erosion events occur on days 305 and 354 (figure 12). For day 305, soil is not frozen, and soil erodibility is high because of recent preplanting tillage, so the rainfall event generates much runoff and a high erosion rate (figure 12b). For day 354, the snowmelt event produces a small erosion event—although the snowmelt runoff is similar in quantity to that on day 305, the lower erodibility (figure 12c) results in less erosion.

Figure 5

Average erosion by (a) slope (S1 [0% to 5%]; S2 [5% to 10%]; S3 [10% to 20%]; S4 [20% to 40%]; and S5 [>40%]), (b) soil depth, (c) tillage, and (d) rotation. Length of each colored bar shows average erosion by the associated class of the factor for the county.

Figure 6

Average erosion in Whitman County weighted by county-level fractions of tillage types (intense, reduced, and no-till) following USDA National Agricultural Statistics Service (NASS) data. Slope (S1 [0% to 5%]; S2 [5% to 10%]; S3 [10% to 20%]; S4 [20% to 40%]; and S5 [>40%]), and precipitation zone (low [<380 mm y^{-1}]; intermediate [380 to 460 mm y^{-1}]; and high [>460 mm y^{-1}]).
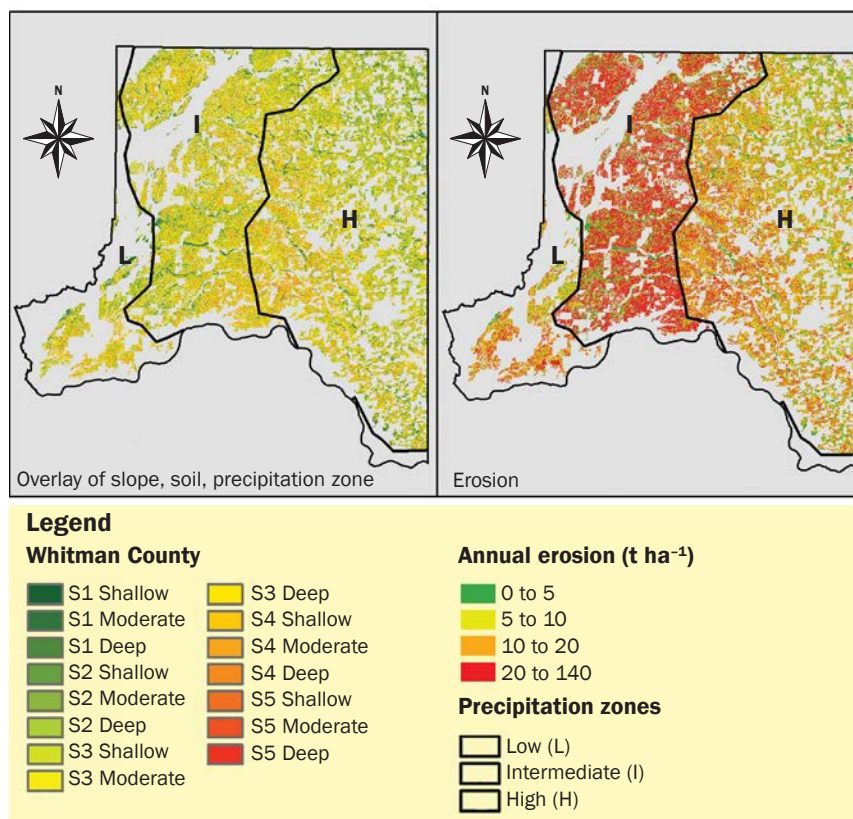

Overlay of slope, soil, precipitation zone | Erosion

Legend

Whitman County

- S1 Shallow
- S1 Moderate
- S1 Deep
- S2 Shallow
- S2 Moderate
- S2 Deep
- S3 Shallow
- S3 Moderate
- S3 Deep
- S4 Shallow
- S4 Moderate
- S4 Deep
- S5 Shallow
- S5 Moderate
- S5 Deep

Annual erosion (t ha^{-1})

- 0 to 5
- 5 to 10
- 10 to 20
- 20 to 140

Precipitation zones

- Low (L)
- Intermediate (I)
- High (H)

Figure 7

Annual area weighted erosion rate in Whitman County (1989 to 2018) for different precipitation zones (low [<380 mm y^{-1}]; intermediate [380 to 460 mm y^{-1}]; and high [>460 mm y^{-1}]).

Legend

- High-precipitation zone
- Intermediate-precipitation zone
- Low-precipitation zone
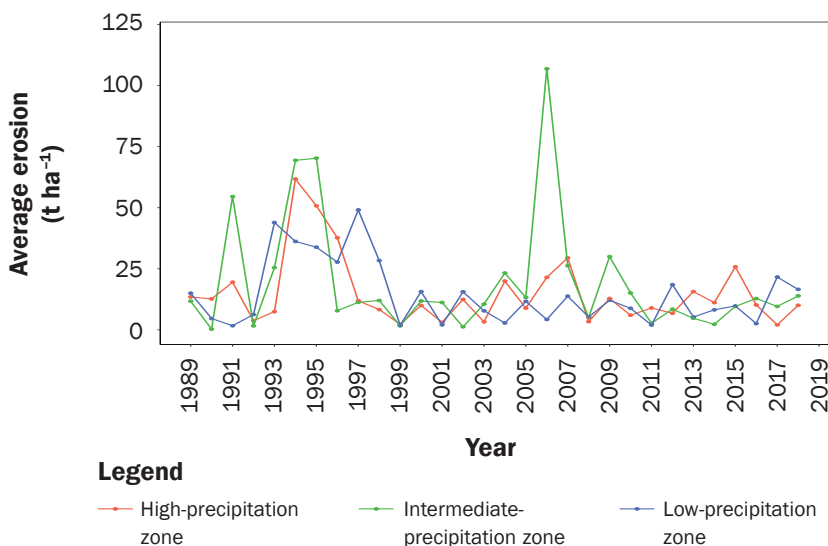
It should be noted that WEPP hillslope version only estimates sheet and rill erosion on hillslopes; channel erosion was not examined in this study. Dynamic soil properties in WEPP, such as K_h and erodibility, change with season and rotation, due to the effect of management operations (e.g., tillage, seeding) and winter processes, especially soil freeze-thaw. Without calibration, current adjustment of the parameter values would have underestimated erosion rates reported for the study area. Additional analysis (including uncertainty assessment) and more realistic characterization of these dynamic parameters will improve WEPP's performance.

Summary and Conclusions

In this study, we used the WEPP model (ver. 2012.8) to evaluate how processes in hillslope hydrology and soil erosion by water are influenced by key environmental factors (soil, climate, and topography) and management practices (tillage and crop rotation). The WEPP simulations allowed assessment of the spatial and temporal variation of water erosion in the cereal grain cropland across 12 eastern Washington counties of the inland PNW.

Major environmental factors (five slope classes and three soil depth classes) were classified and overlain with three precipitation zones to define subareas of unique combinations of factor levels within the simulated area. Including the management factor of tillage intensity (three levels) led to a total of 135 (5 × 3 × 3 × 3) scenarios. County-level input files were compiled from the literature, SSURGO, and WEPP databases. Major WEPP simulation outputs, including annual water balance, winter hydrological events, and erosion rates (event, annual, and 30-year average), were evaluated and compared for each county and each precipitation zone to elucidate effects of the environmental and management factors. Geographic information system (GIS) maps of WEPP-simulated erosion rates for the 12 counties display the spatial variability as affected by topography, soil depth, crop rotation, and tillage intensity, revealing "hotspots" where erosion rates are high. Additionally, simulation outputs for Whitman County were examined in more detail and compared with literature findings. Based on WEPP simulation results, we conclude the following:

1. The intermediate–precipitation zone (380 to 460 mm y^{-1}) generates the high-

Figure 8

Runoff by crop rotation ([a] through [c] is winter wheat–barley–pea; [d] through [f] is winter wheat–barley–fallow; and [g] through [i] is winter wheat–fallow), tillage, soil depth, and slope (S1 [0% to 5%]; S2 [5% to 10%]; S3 [10% to 20%]; S4 [20% to 40%]; and S5 [>40%]), Whitman County. (a), (d), and (g) are under intense tillage; (b), (e), and (h) are under reduced tillage; and (c), (f), and (i) are under no-till.
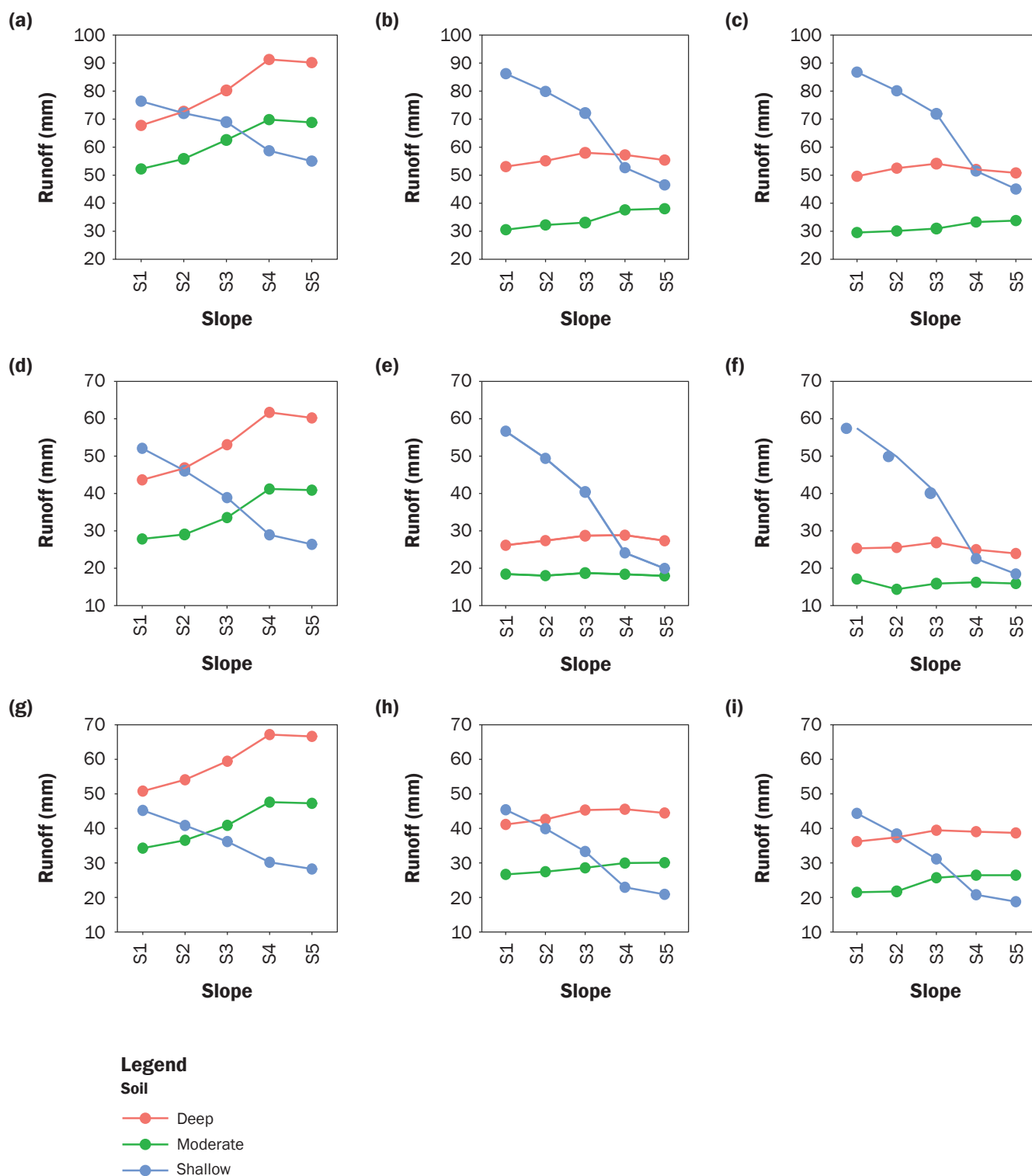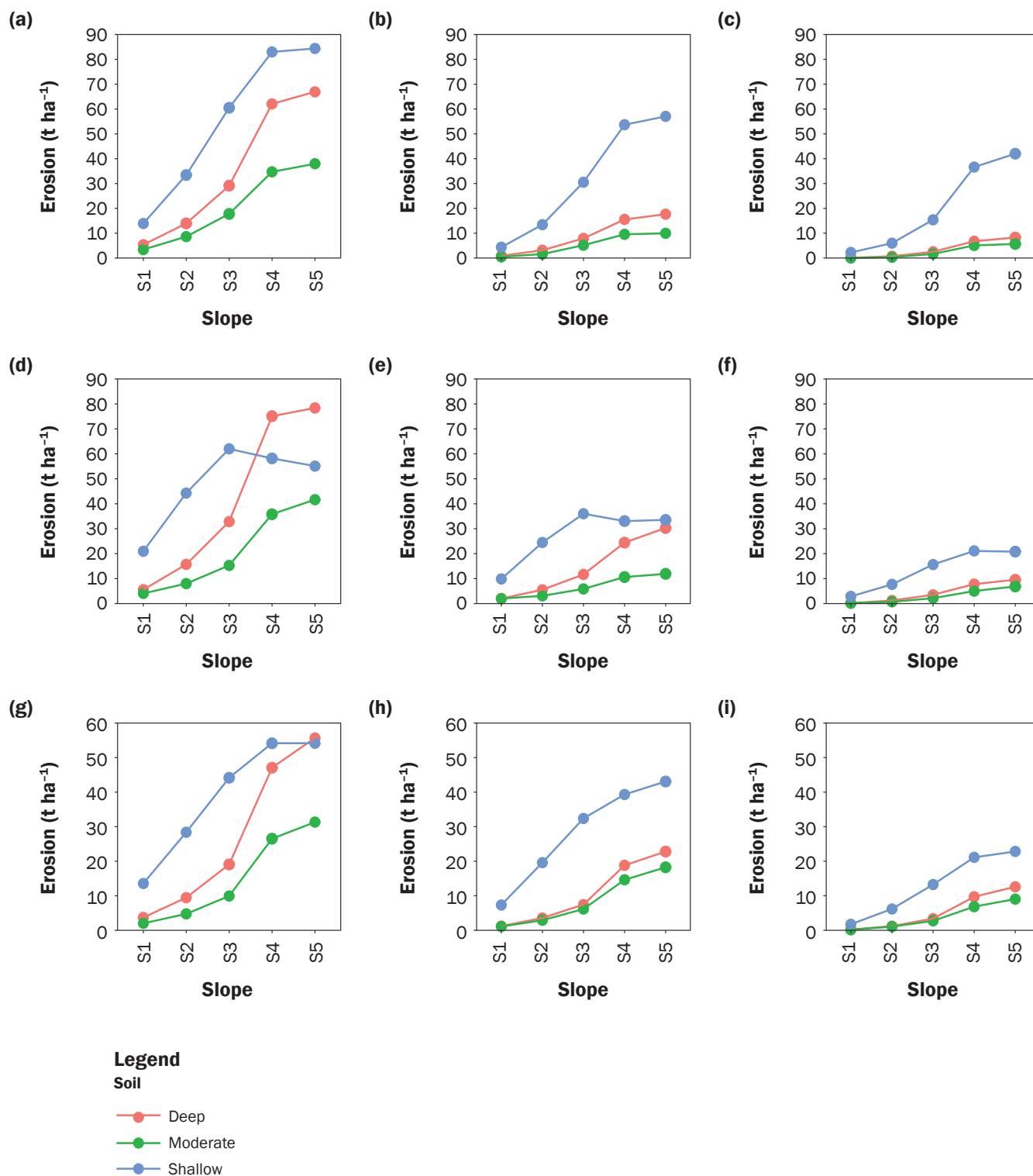
Figure 9

Erosion by crop rotation ([a] through [c] is winter wheat–barley–pea; [d] through [f] is winter wheat–barley–fallow; and [g] through [i] is winter wheat–fallow), tillage, soil depth, and slope (S1 [0% to 5%]; S2 [5% to 10%]; S3 [10% to 20%]; S4 [20% to 40%]; and S5 [>40%]), Whitman County. (a), (d), and (g) are under intense tillage; (b), (e), and (h) are under reduced tillage; and (c), (f), and (i) are under no-till.

est erosion rates and high amount of erosion at 4.2×10^6 t y^{-1}, despite having the smallest area among the three precipitation zones. Erosion rates in many cases exceed the USDA tolerable limit for soil loss. Erosion rates are lowest in the low-precipitation zone (<380 mm y^{-1}) due to the lower runoff generated. However, even in counties with low average erosion rates, erosion rates in the "hotspots" could be five times greater than the average for that county.

2. Under similar climatic conditions, erosion is greater during the fallow and wheat-planting years because the bare soil during the fallow period renders the soil more prone to erosion, and soil erodibility increases due to preplanting tillage during the wheat year.

3. Areas with steeper slopes, relatively higher precipitation on unprotected soil, and more intense tillage combine to result in high erosion. Whitman, Garfield, and Columbia counties have among the highest average erosion rates, and all three counties have relatively large area with steep terrain and intense tillage. In contrast, Walla Walla County, with a similar topography, produces lower erosion because the percentage area under intense tillage in the county is lower.

4. Shallow soils on less steep slopes in the study area tend to produce larger erosion rates because of their greater tendency for saturation-excess runoff, as compared to the moderately deep and deep soils. In counties such as Garfield and Whitman, shallow soils with relatively low hydraulic conductivity conducive to infiltration-excess runoff, combined with steeper slopes and intense tillage, yield markedly high erosion.

5. In Whitman County's low-, intermediate-, and high-precipitation zones, 59%, 57%, and 54% of the areas have erosion rates greater than the NRCS tolerable limit of soil loss. Prioritizing conservation practices in these erosion hotspots would increase implementation efficiency and effectiveness.

6. Conservation measures will be especially effective at decreasing erosion if they are applied to the fallow and wheat-planting years. For example, replacing fallow with cover crops will substantially reduce soil erosion.

7. Limitations in this study include: tillage practice data reported at county level were used for subareas within the county, percentage areas of specific tillage types reported for all crops were assumed to apply to cereal grain crops, designation of wheat as the crop for the first simulation year, and calibration of dynamic parameters based primarily on limited reported soil erosion data. Results of this study should therefore be taken with caution.

Supplemental Material

The supplementary material for this article is available in the online journal at https://doi.org/10.2489/jswc.2022.00091.

Acknowledgements

References

Ayalew, H., T.T. Kumssa, T. Butler, and X.-F. Ma. 2018. Triticale improvement for forage and cover crop uses in the southern Great Plains of the United States. Front Plant Science 9:1130. https://doi.org/10.3389/fpls.2018.01130.

Boll, J., E.S. Brooks, B. Crabtree, S. Dun, and T.S. Steenhuis. 2015. Variable source area hydrology modeling with the Water Erosion Prediction Project model. Journal of the American Water Resources Association 51:330–342.

Brooks, E.S., S.M. Saia, J. Boll, L. Wetzel, Z.M. Easton, and T.S. Steenhuis. 2015. Assessing BMP effectiveness and guiding BMP planning using process-based modeling. Journal of American Water Resources Association 51:343–358.

Busacca, A.J. 1989. Long quaternary record in eastern Washington, U.S.A. interpreted from multiple buried paleosols in loess. Geoderma 45:105–122.

Cochran, V.L., L.F. Elliott, and R.I. Papendick. 1982. Effect of crop residue management and tillage on water use efficiency and yield of winter wheat. Agronomy Journal 74:929–932.

Figure 10

Annual precipitation and erosion rates for the scenario of high-precipitation zone, S3 slope, deep soil, intense tillage, in Whitman County.
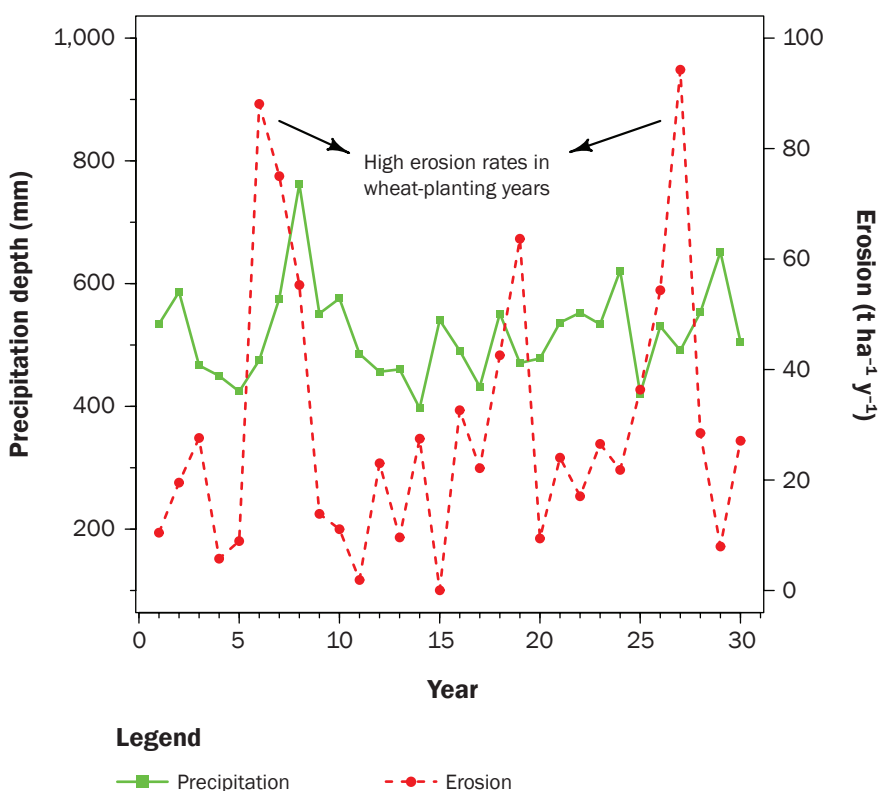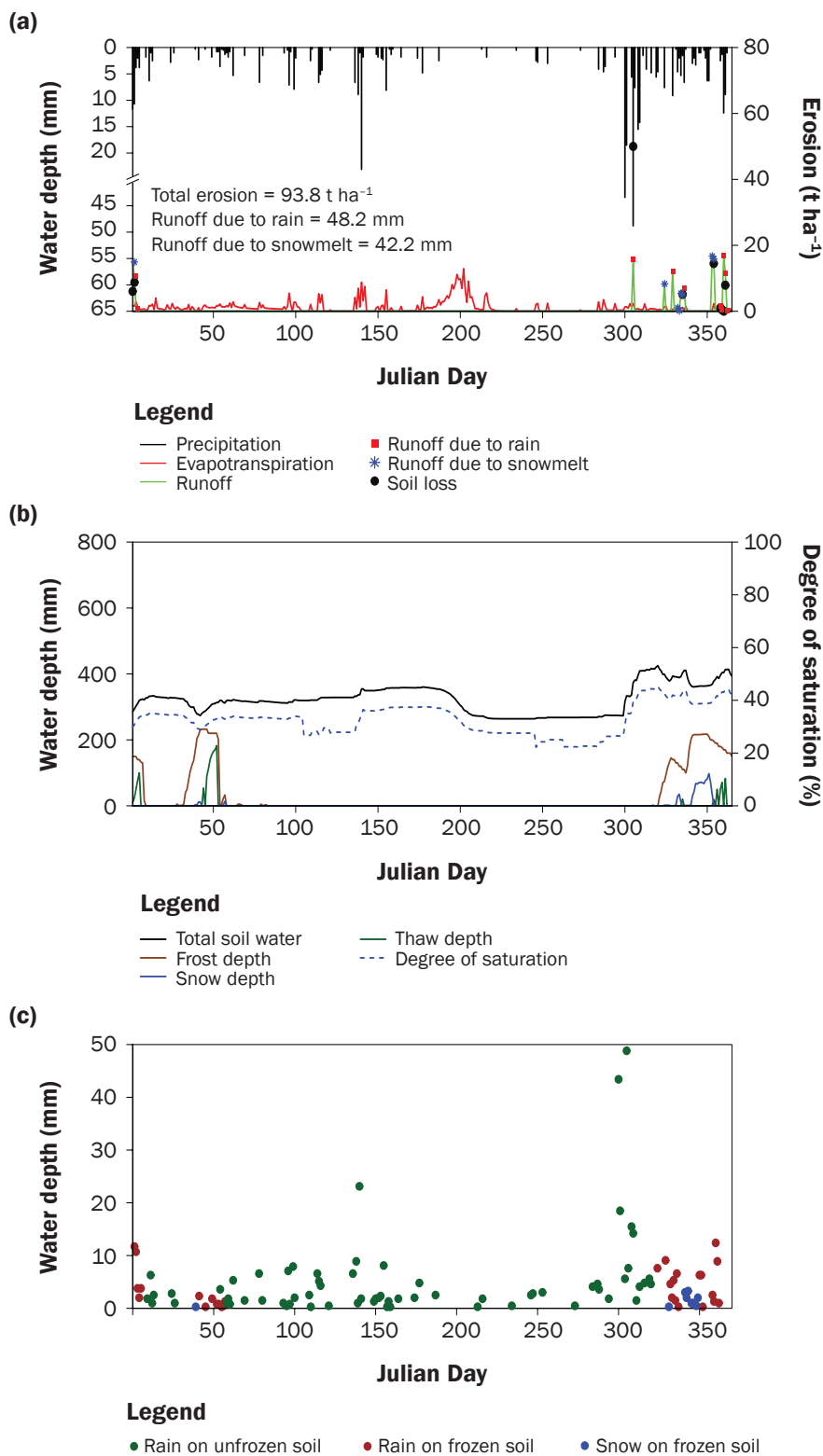
Figure 11

Daily water balance and erosion detail of simulation year 6 for the scenario of high-precipitation zone, S3 slope, deep soil, intense tillage, in Whitman County. (a) Water balance, (b) soil profile conditions, and (c) precipitation type and amount.

DiNezio, P.N., C. Deser, Y. Okumura, and A. Karspeck. 2017. Predictability of 2-year La Niña events in a coupled General Circulation Model. Climate Dynamics 49:4237–4261. https://doi.org/10.1007/s00382-017-3575-3.

Domenico, P.A., and F.W. Schwartz. 1997. Hydraulic conductivity and permeability of geologic materials. *In* Physical and Chemical Hydrogeology. New York: John Wiley & Sons Inc.

Dun, S., J.Q. Wu, W.J. Elliot, P.R. Robichaud, D.C. Flanagan, J.R. Frankenberger, R.E. Brown, and A.C. Xu. 2009. Adapting the Water Erosion Prediction Project (WEPP) model for forest applications. Journal of Hydrology 366:46–54.

Dun, S., J.Q. Wu, D.K. McCool, J.R. Frankenberger, and D.C. Flanagan. 2010. Improving frost simulation subroutines of the Water Erosion Prediction Project (WEPP) model. Transactions of the ASABE 53:1399–1411.

ESRI (Environmental Systems Research Institute). 2019. ArcGIS Desktop: Release 10.7.1. Redlands, CA: Environmental Systems Research Institute.

Flanagan, D.C., and S.J. Livingston, ed. 1995. USDA–Water Erosion Prediction Project User Summary. National Soil Erosion Research Laboratory Report No. 11. West Lafayette, IN: USDA Agricultural Research Service, National Soil Erosion Research Laboratory.

Flanagan, D.C., and M.A. Nearing, ed. 1995. USDA–Water Erosion Prediction Project Hillslope Profile and Watershed Model Documentation. National Soil Erosion Research Laboratory Report No. 10. West Lafayette, IN: USDA ARS National Soil Erosion Research Laboratory.

Ghimire, R., B. Ghimire, A.O. Mesbah, O.J. Idowu, M.K. O'Neill, S.V. Angadi, and M.K. Shukla. 2018. Current status, opportunities and challenges of cover cropping for sustainable dryland farming in the Southern Great Plains. Journal of Crop Improvement 32:579–598.

Greer, R.C., J.Q. Wu, P. Singh, and D.K. McCool. 2006. WEPP simulation of observed winter runoff and erosion in the Pacific Northwest, USA. Vadose Zone Journal 5:261–272.

Hill, W.W., and V.G. Kaiser. 1965. Method of measuring soil erosion losses: Rill and sheet erosion. Soil Survey Technical Notes: 13–14. Washington, DC: USDA Soil Conservation Service.

Hudson, N. 1993. Field measurement of soil erosion and runoff. Soils Bulletin 68. Rome: Food and Agricultural Organization of the United Nations.

Huggins, D., B. Pan, W. Schillinger, F. Young, S. Machado, and K. Painter. 2015. Crop diversity and intensity in Pacific Northwest dryland cropping systems. *In* Regional Approaches to Climate Change for Pacific Northwest Agriculture (REACCH PNA)—Climate Science Northwest Farmers Can Use, ed. K. Borrelli, D.D. Laursen, S. Eigenbrode, B. Mahler, and R. Pepper. Moscow, ID: REACCH PNA. www.reacchpna.org.

Kirby, E.M., W.L. Pan, D.R. Huggins, K.M. Painter, and P. Bista. 2017. Rotational diversification and intensification. *In* Advances in Dryland Farming in the Inland Pacific Northwest, ed. G. Yorgey and C. Kruger, 163–236. Pullman, WA: Washington State Extension Publication EM108–05.

Kok, H., R.I. Papendick, and K.E. Saxton. 2009. STEEP: Impact of long-term conservation farming research and education in Pacific Northwest Wheatlands. Journal of Soil and Water Conservation 64(4):253–264. https://doi.org/10.2489/jswc.64.4.253.

Kottek, M., J. Grieser, C. Beck, B. Rudolf, and F. Rubel. 2006. World map of the Köppen-Geiger climate classification updated. Meteorologische Zeitschrift 15:259–263. doi:10.1127/0941-2948/2006/0130.

Lal, R. 1998. Soil erosion impact on agronomic productivity and environment quality. Critical Reviews in Plant Science 17:319–464.

Langdale, G.W., R.L. Blevins, D.L. Karlen, D.K. McCool, M.A. Nearing, E.L. Skidmore, A.W. Thomas, D.D. Tyler, and J.R. Williams. 1991. Cover crop effects on soil erosion by wind and water. *In* Cover Crops for Clean Water, ed. W.L. Hargrove, 15–21. Ankeny, IA: Soil and Water Conservation Society.

Matsuura, K., C. Willmott, and D. Legates. 2021. WebWIMP v.1.02. https://davinci.geog.udel.edu/~wimp/.

McCool, D.K., and R.D. Roe. 2005. Long-term erosion trends on cropland in the Pacific Northwest. Presented at American Society of Agricultural Engineering Annual Meeting. Paper number: PNW05-1002. St Joseph, MI: American Society of Agricultural Engineers.

Meyer, L.D. 1982. Soil erosion research leading to development of the universal soil loss equation. *In* Proceedings of Workshop on Estimating Erosion and Sediment Yield on Rangelands, ed. G.R. Foster, 1–16. Washington, DC: USDA Agricultural Research Service.

Montanarella, L. 2015. Agricultural policy: Govern our soils. Nature 528:32–33.

Montgomery, D.R. 2007. Soil erosion and agricultural sustainability. Proceedings of the National Academy of Sciences of the United States of America 104:13268–13272.

Mulla, D.J., A.S. Birr, N.R. Kitchen, and M.B. David. 2008. Limitations of evaluating the effectiveness of agricultural management practices at reducing nutrient losses to surface waters. *In* American Society of Agricultural and Biological Engineers, Final Report: Gulf Hypoxia and Local Water Quality Concerns Workshop, 189–212. St. Joseph, MI: American Society of Agricultural and Biological Engineers.

NCDC (National Climatic Data Center). 2018. NOAA satellite and information service. Asheville, NC: NCDC. https://www.ncdc.noaa.gov/cdo-web/.

Nicks, A.D., L.J. Lane, and G.A. Gander. 1995. Weather generator. *In* USDA-Water Erosion Prediction Project: Hillslope profile and watershed model documentation, ed. D.C. Flanagan and M.A. Nearing, 2.1–2.22. NSERL

Figure 12

Comparison of events on days 305 and 354, simulation year 6, for the scenario of high-pre-cipitation zone, S3 slope, deep soil, intense tillage, in Whitman County. (a) Water balance, (b) water in soil profile and erosion, and (c) erodibilities and critical shear adjusted daily for factors including canopy cover, residue, and freeze and thaw. The results in (b) and (c) are for the first soil layer.
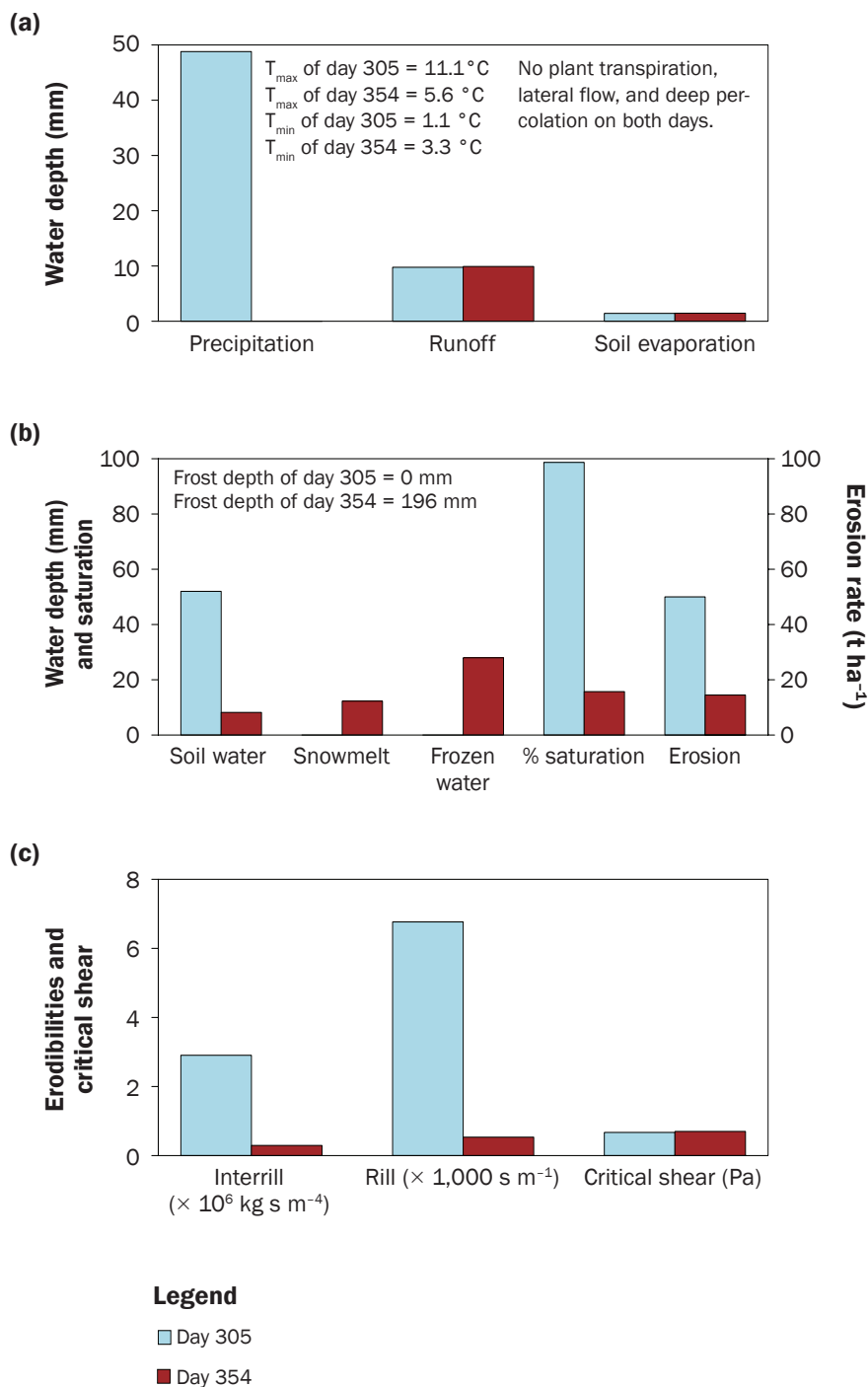
Report 10. West Lafayette, IN: National Soil Erosion Research Laboratory.

Nielsen, D.C., D.J. Lyon, and J.J. Miceli-Garcia. 2017. Replacing fallow with forage triticale in a dryland wheat-corn-fallow rotation may increase profitability. Field Crops Research 203:227–237. doi:10.1016/j.fcr.2016.12.005.

Oldenstadt, D.L., R.E. Allan, G.W. Bruehl, D.A. Dillman, E.L. Michalson, R.I. Papendick, and D.J. Rydrych. 1982. Solutions to Environmental and Economic Problems (STEEP). Science 217:904–909.

Papendick, R.I., F.L. Young, K.S. Pike, and R.J. Cook. 1995. Description of the region. *In* Crop Residue Management to Reduce Erosion and Improve Soil Quality: Northwest, CRR-40, ed. R.I. Papendick and W.C. Moldenhauer. Washington, DC: USDA ARS.

Pieri, L., M. Bittelli, J.Q. Wu, S. Dun, D.C. Flanagan, P.R. Pisa, F. Ventura, and F. Salvatorelli. 2007. Using the Water Erosion Prediction Project (WEPP) Model to simulate field-observed runoff and erosion in the Apennines Mountain Range, Italy. Journal of Hydrology 336:84–97.

Shepherd, J.F. 1985. Soil conservation in the Pacific Northwest wheat-producing areas: Conservation in a hilly terrain. Agricultural History 59:229–245.

Singh, V.P. 1995. Computer Models of Watershed Hydrology. Water Resources Publications, Highlands Ranch, CO: Water Resources Publications.

Singh, P., J.Q. Wu, D.K. McCool, S. Dun, C.-H. Lin, and J.R. Morse. 2009. Winter hydrological and erosion processes in the US Palouse region: Field experimentation and WEPP simulation. Vadose Zone Journal 8:426–436.

Soil Science Division Staff. 2017. Soil Survey Manual. *In* USDA Handbook 18, ed. C. Ditzler, K. Scheffe, and H.C. Monger. Washington, DC: Government Printing Office. https://www.nrcs.usda.gov/wps/portal/nrcs/detail/soils/scientists/?cid=nrcs142p2_054262.

Soil Survey Staff. 2019. Web Soil Survey. Washington, DC: USDA Natural Resources Conservation Service. http://websoilsurvey.sc.egov.usda.gov/.

Tang, Y., R.H. Zhang, T. Liu, W. Duan, D. Yang, F. Zheng, H. Ren, T. Lian, C. Gao, D. Chen, and M. Mu. 2018. Progress in ENSO prediction and predictability study. National Science Review 5:826–839. https://doi.org/10.1093/nsr/nwy105.

Taylor, G.H. 1998. Impacts of the El Niño Southern Oscillation on the Pacific Northwest. Oregon Geology 60:51–56. http://citeseerx.ist.psu.edu/viewdoc/download? doi=10.1.1.643.1390&rep=rep1&type=pdf#page=51.

USDA. 1978. Palouse Cooperative River Basin Study. Washington, DC: USDA Soil Conservation Service, Forest Service, and Economics, Statistics, and Cooperative Service.

USDA. 2020. Summary Report: 2017 National Resources Inventory. Washington, DC, and Ames, IA: Natural Resources Conservation Service, and Center for Survey Statistics and Methodology, Iowa State University.

USDA NASS (National Agricultural Statistics Service). 2017. Census of Agriculture. Washington, DC: USDA NASS. www.nass.usda.gov/AgCensus.

USDA NASS. 2018. 2018 Washington Cropland Data Layer. Washington, DC: USDA NASS. https://nassgeodata.gmu.edu/CropScape/.

USDA NRCS (USDA Natural Resources Conservation Service). 2020. Honoring 85 Years of NRCS—A Brief History. Washington, DC: USDA NRCS. https://www.nrcs.usda.gov/wps/portal/nrcs/detail/national/about/history/?cid=nrcs143_02132.

USGS (US Geological Survey). 2019. USGS NED 1 arc-second ArcGrid 2019. Reston, VA: USGS. https://apps.nationalmap.gov/downloader/.

Van Klaveren, R.W., and D.K. McCool. 1998. Erodibility and critical shear of a previously frozen soil. Transactions of the ASAE 41:1315–1321.

Williams, J.D., S. Dun, D.S. Robertson, J.Q. Wu, E.S. Brooks, D.C. Flanagan, and D.K. McCool. 2010. WEPP simulations of dryland cropping systems in small drainages of Northeastern Oregon. Journal of Soil and Water Conservation 65(1):22–33. https://doi.org/10.2489/jswc.65.1.22.

Wischmeier, W.H., and D.D. Smith. 1978. Predicting Rainfall Erosion Losses: A Guide to Conservation Planning. USDA, Agriculture Handbook Number 537. Washington, DC: US Government Printing Office.

Zhang, C., J.-J. Luo, and S. Li. 2019. Impacts of tropical Indian and Atlantic Ocean warming on the occurrence of the 2017/2018 La Niña. Geophysical Research Letters 46:3435–3445.